IJCRT.ORG ISSN : 2320-2882

INTERNATIONAL JOURNAL OF CREATIVE RESEARCH THOUGHTS (IJCRT)

An International Open Access, Peer-reviewed, Refereed Journal

DYNAMICS OF LAND COVER INDICES AND THEIR RELATION WITH URBAN BIOPHYSICAL COMPONENT OF KANPUR METROPOLIS IN THE GANGA-YAMUNA DOAB REGION OF INDIA

[1]Himanshu Gandhi, [2]G.L. Srivastava [3]Vikram Gauarv Singh, [4]Shiv Bahadur Singh, [5]Vinay Kumar
[1]Research Scholar, [2]Professor, [3]Coordinator, [4]Research Scholar, [5]Research Scholar

[1]Department of Geography. [2]Department of Geography, [3]Source Sustainability at State Water and Sanitation Mission UP, [4]Department of Geography, [5]Department of Geography

[1]DAV Degree College, Kanpur, India, [2]DAV Degree College, Kanpur, India, [3]Aga Khan Foundation, Lucknow, India, [4]VSSD College, Kanpur, India, [5]DAV Degree College, Kanpur, India

Abstract: Land Cover Indices gives information about the thermal behavior of land surfaces and when it coincide with sensible heat storage (ΔQ_S) then it forms urban heat island which in turn measure in its intensity. The current study analyzed the effects of land cover indices in the Kanpur Metropolis, which is located over the Indo Gangetic Plains but now a portion of the Kanpur Nagar District and has the Yamuna river as its southern boundary due to its urban sprawl. The land cover indices such as Modified Normalized Difference Water Index (MNDWI), Normalized Difference Barren index (NDBaI), Normalized Difference Built-up Index (NDBI), Difference Vegetation Index (NDVI) Soil Adjusted Vegetation Index (SAVI) affects Urban Heat Island (UHI) intensity. These land cover indices and Urban Heat Island (UHI) intensity has been calculated using data from Landsat 5, 7, and 8 for the years 1991, 2001, 2011, and 2021respectively for this region using projection WGS_1984_UTM_Zone_44N. A correlation between UHI Intensity and various land cover indices has also been evaluated, and it reveals that NDBI and NDBaI have a positive impact on UHI Intensity while MNDWI, NDVI, and SAVI have a negative impact. The UHI intensity is positively correlated with NDBaI and NDBI according to the best fit curve with a logarithmic trendline, but it is negatively correlated with MNDWI, NDVI, and SAVI. The significance level (p) for each land cover index was also evaluated, and in the majority of cases, a satisfactory p value of <.05 was discovered. The analysis demonstrates that while the land cover indices associated with vegetation density the Urban Heat Island Intensity has decreased in the region while indices associated with built-up such as NDBI, the UHI Intensity has increased. The study can offer insightful information about the policy-making process for urban spatial planning and strategies to mitigate UHI Intensity.

Keywords: Landsat, land use indices, urban heat island intensity.

Introduction: More than half of the world's population (55%) currently residing in urban areas and this number is expected to rise upto 68% by the year 2050 in today's more connected and globally oriented world (UN, 2019). Urban sprawl has been exacerbated by the speed and scope of widespread Land Use and Land Cover Change (LULCC), which has been brought on by the rising demands for food, energy, water, fiber, and shelter from the expanding human population. Urbanization drastically changed the natural landscape around the world by converting naturally permeable land surfaces into impervious ones (urban landscape) (Scott J. McGrane, 2016; Paul et al., 2021). A change in the natural terrestrial cover affects the earth's surface's radiative and non-radiative properties, carbon dynamics, and biogeochemical processes, which in turn alters the water cycle and the local environment (Duveiller et al., 2018). A number of environmental problems are brought on by the conversion of natural terrestrial cover into built-up land-use (urban landscape) (Jed Collins 2019; M. Hanif et al., 2019), including the emergence of micro-thermal and micro-climatic zones (K.A.S. Mislan & B. Helmuth, 2008; K.K. Singh et al., 2018), an increase in land surface temperature (LST), and urban heat islands (UHI) intensity (Amit Kumar et al., 2021; B.P. Kumar et. al., 2023). The land cover indices based on subpixel classification (Zhang et al., 2006;Weng et. al., 2008) the various classification based on indices such as The Normalized Difference Vegetation Index (NDVI), Soil Adjusted Vegetation Index (SAVI), Modified Normalized Difference Water Index (MNDWI), Normalized Difference Bareness Index (NDBaI), and Normalized Difference Build-up Index (NDBI) suggest about land occupancy by different characteristic and different sensible and latent heat fluxes (Hui Li et al., 2017; Dan Li et al., 2020) and these land indices also provides rapid surface heat island detection due to their characteristics (Nagihan Aslan and Dilek-Koc-San, 2021) and with such a few of these land cover indices that LST interacts with to characterize the thermal behavior of the land surfaces (G. Duveiller et al., 2018; Z.L. Li et al., 2018; Glynn C. Hulley et al., 2019). However, LST changes as a result of the conversion of the natural terrestrial cover to impervious surfaces (urban landscape) which affects UHI Intensity.

The term "urban heat island" (UHI) describes the phenomenon of sensible heat storage (ΔQ_S) due to which cities experience higher atmospheric and surface temperatures than the nearby rural areas as a result of urbanization. It is related to the arrangement and pattern of land-use types, as well as landscape features (Qingjian Zhao et al., 2019; Alademomi Alfred S. et al., 2020), the composition of LULC in urban areas affects the thermal conductivities of urban surfaces (Mustafa Hamoodi et al., 2017; Ayansina Ayanlade et al., 2021). The amount of vegetation present within a city (Lei Zhang et al., 2022), anthropogenic discharge from human activities and built-up density affects ecological system and reflects ecological environment (Dingrao Feng et al., 2020). The urban canopy, which is the layer between the ground and building rooftops, and which is strongly influenced by surface, morphological, and anthropic parameters (Florent Renard et al., 2019; Junyan Yang, 2020) which in turn gives three distinct UHI types and on the basis of sensible heat flux (Δf_S) quantity that are typically distinguished as: 1. canopy UHII, 2. boundary-layer UHII, and 3. surface UHII. Just above the canopy layer is the boundary layer, which is influenced by both the mesoscale processes that occur above it as well as the microscale processes that occur beneath it (J.S.M. Coleman and K.T. Law, 2015; D.J. Parker, 2015; Stefano Serafin et al., 2018). The study of surface UHII, which is based on the measurement of land-surface temperatures (LST), which directly affect air temperature in the canopy layer by energy exchange and forms the Urban Heat Island effect (Nidhi Singh et al., 2020; Manju Mohan et al., 2022). Currently, researchers from all over the world uses satellite thermal images, particularly high resolution images, to study thermal anomalies like UHI intensity in urban areas (Ana Claudia Teodoro and Artur Goncalves 2021). These images have the advantage of offering a repeatable dense grid of temperature data over an entire city and even distinct temperatures for individual buildings (Yunfei Li et al., 2020; Eric Krause, 2022).

In this light, the main goal of the current study is to quantify and analyze the spatiotemporal patterns of the UHII phenomenon (Pallavi Sharma, 2021) over the Indian district of Kanpur Nagar in the Ganga-Yamuna Doab with common land cover indices. In order to determine which indices have the greatest influence on temperatures, the study also examines the relationship between Urban Heat Island (UHI) intensity and common land cover indices (David Hidalgo Garcia et al., 2023; Waheed Ullah et al., 2023), such as MNDWI, NDBaI, NDBI, NDVI, and SAVI, using Earth Observation (EO) datasets and a quantitative approach based on geospatial technology (GT). Finding the factors that affect heat scenarios is crucial because doing so we can lowers the impact of UHII and boosts the quality of the urban environment. Designing of urban green and blue spaces can help planning strategies for reducing the effects of UHII in cities of developing nations like India.

2. Materials and Methods:

2.1 Area of Study: In the "Survey of India's" Toposheet Nos. 54N and 63B, the study area Kanpur Nagar (Fig. 1) is situated over north-central India in the middle of the state of Uttar Pradesh between latitudes 25°55'N to 27°N and longitude 79°30'E to 80°35'E. It is one of the Indian cities with a population greater than 4.5 million and is bordered on the north by the Ganga River and on the south by the Pandu River (Yamuna). It is the eleventh most populous urban city in India (according to 2011 census).

The districts of Kanuuaj and Hardoi, Unnao in the east, Fatehpur and Hamirpur in the south, and Kanpur Dehat in the west form its northern, eastern, southern, and western boundaries. It is separated from the districts of Kanpur Dehat and Fatehpur in the west and south, respectively, by the Pandu River, and from the district of Unnao in the east by the holy Ganga River, which acts as a natural barrier. Kanpur Nagar district comes under the "Ministry of Housing and Urban Affairs, Government of India (GoI)". It has a total geographic area of 3180 sq. km, and the city's total area is 403 km^2. The river Ganga and river Yamuna forms the study area's north-east and south-west boundaries, respectively, and develop the fertile agricultural hinterland of Ganga and Yamuna Doab. It has a population of 4.58 million and a population density of 6850 people per km^2 (District Census Handbook, 2011), The study area has an average elevation of 125 meters above mean sea level and is located on a nearly level plain with a few minor undulations, with the master slope running from the northwest to the south-east while river Ganga and river Yamuna makes district's climate sub-humid and it is characterized by hot summers and general dryness save for the south-west monsoon, having an average annual rainfall of 821.9 mm. The average monthly maximum temperature in the district is 32.2°C, while the average monthly minimum temperature is 19.5°C. The main sedimentary constituents of the soil are clay, silt, gravel, and sands of various grades. The district also enjoys strong administration and has good range of all facilities for its people.

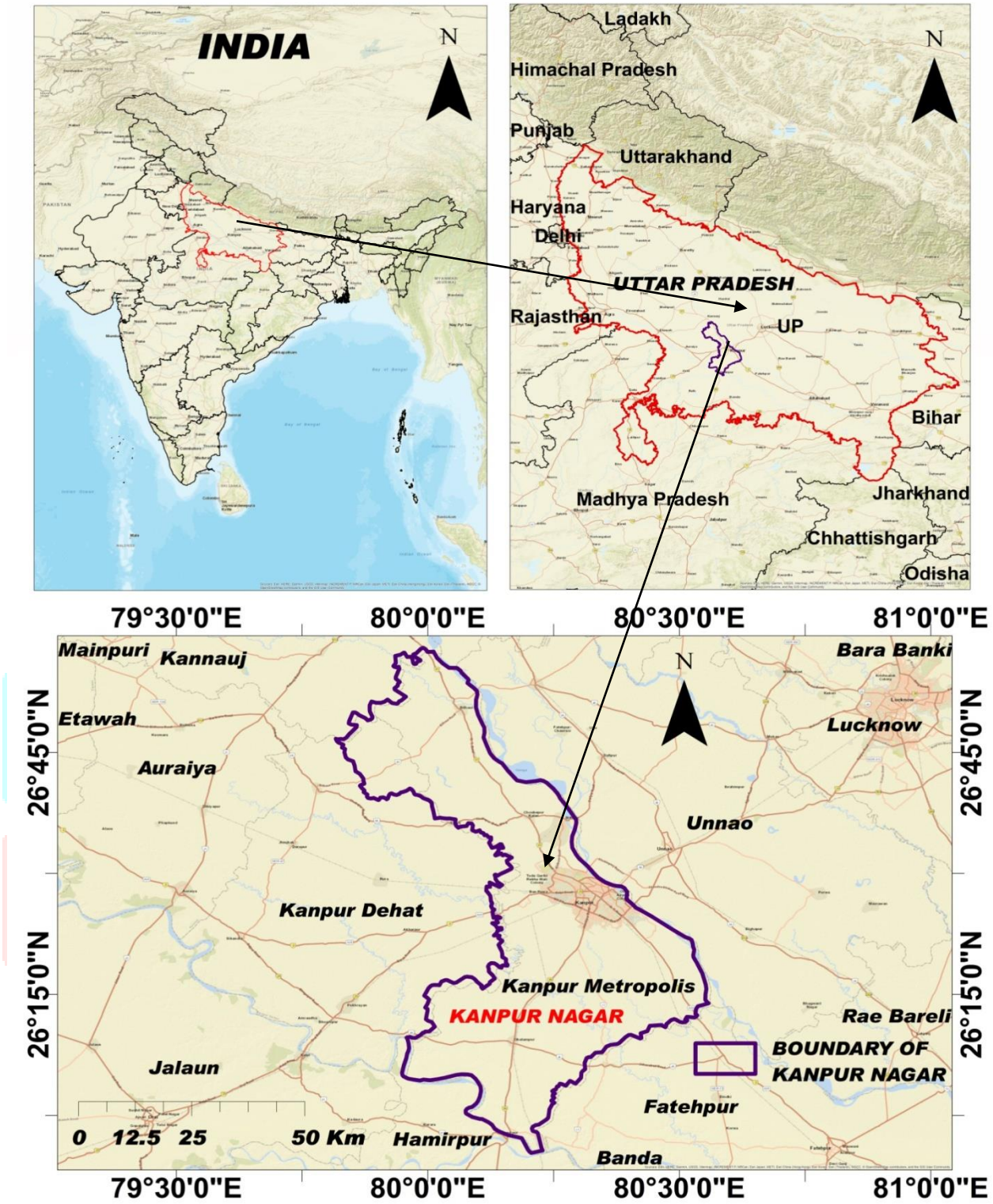

Figure 1

Figure 1 shows the district boundary of Kanpur Nagar and its surrounding areas.

2.2 Data: From the US Geological Survey's website, https://earthexplorer.usgs.gov/, path 144 and rows 041 and 042 of Landsat5, Landsat7, and Landsat8 data are downloaded. The data are then mosaiced, and ArcMap 10.8 software is used to extract data for the region.

Here are the specifics of the used satellite images

Satellite	Sensor	Acquisition date	Path and row	Spatial resolution	Thermal resolution	Cloud Cover
Landsat 5	TM	16 March 1991	144/041 & 144/042	30 m	120(30)m	<10%
Landsat 7	ETM+	03 March 2001	144/041 & 144/042	30 m	60(30)m	<10%
Landsat 5	TM	07 March 2011	144/041 & 144/042	30 m	120(30)m	<10%
Landsat 8	OLI/TIRS	02 March 2021	144/041 & 144/042	30 m	100m	<10%

Table-1

The UHI and land cover indices were extracted from satellite images from the Landsat series in this study, and the year-by-year values of UHI Intensity were compared with the MNDWI, NDBaI, NDBI, NDVI, and SAVI indices. The methodology flow chart (Figure 2) gives a detailed explanation of the steps taken in the study.

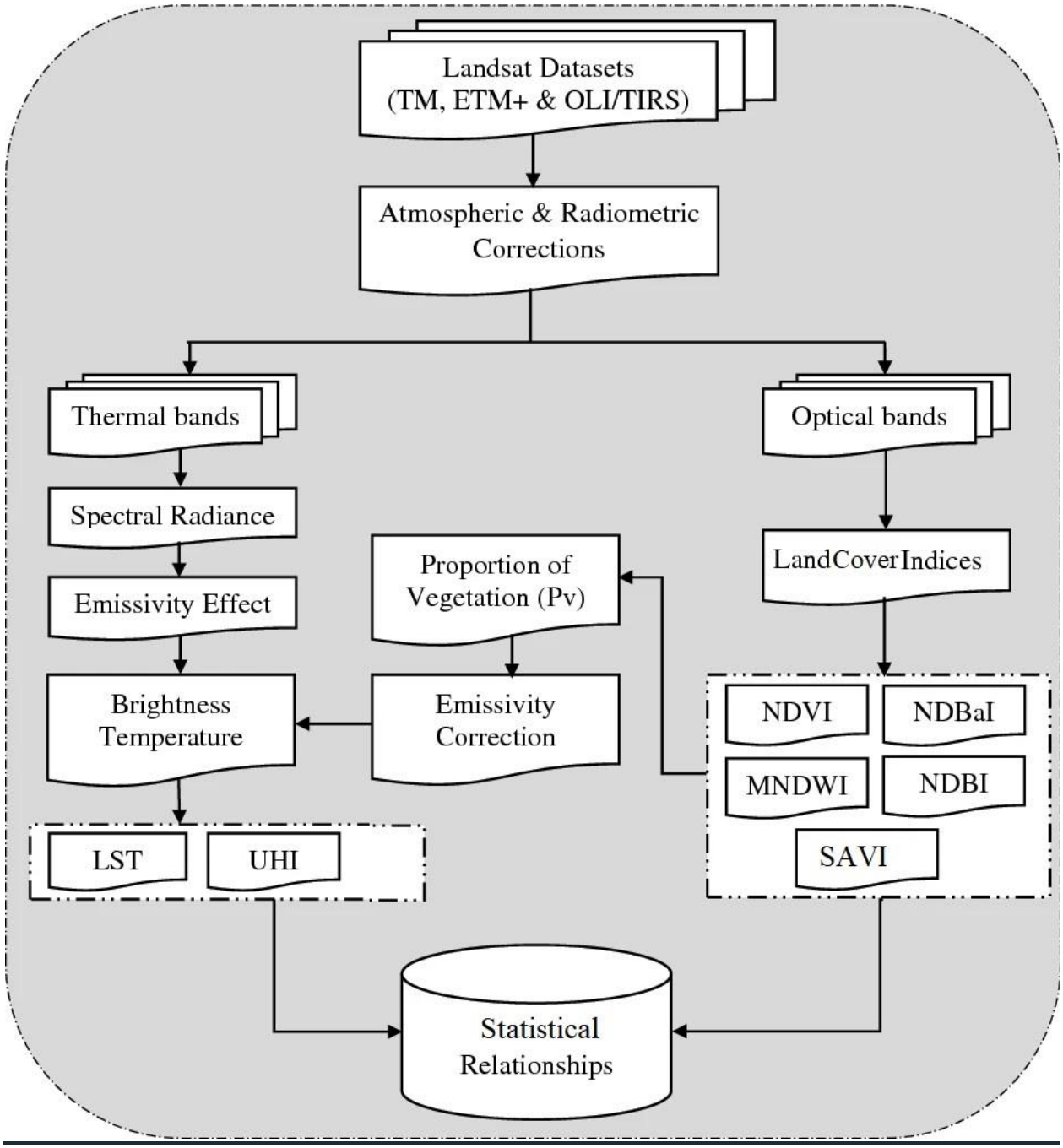

Figure 2

2.3.1 Land Cover Indices

The Normalized Difference Bareness Index (NDBaI) recognizes various types of bare areas, while the Modified Normalized Difference Water Index (MNDWI) is used to improve open water features. The Normalized Difference Vegetation Index (NDVI), which is used to measure vegetation greenness and is helpful in understanding vegetation density, Normalized Difference Built-up Index (NDBI) emphasizes artificially constructed built-up areas. In areas with little vegetative cover, the Soil Adjusted Vegetation Index (SAVI) is used to measure the impact of soil brightness.

Keeping this in view Zha et al., (2003) proposed the mechanism to derive these indices and according to it, MNDWI, NDBaI, NDBI, NDVI, and SAVI indices can be derived from these formulas:

- MNDWI is equal to (Green – SWIR) / (Green + SWIR)

In the case of Landsat 5,7, MNDWI is equal to float (Band 2 - Band 5)/float (Band 2 + Band 5)

In the case of Landsat 8, MNDWI is equal to float (Band 3 - Band 6)/float (Band 3 + Band 6)

- NDBaI is equal to (SWIR - TIR)/ (SWIR - TIR)

In the case of Landsat 5,7, NDBaI is equal to float (Band 5 - Band 6)/float (Band 5 + Band 6)

In the case of Landsat 8, NDBaI is equal to float (Band 6 - Band 10)/float (Band 6 + Band 10)

- NDBI is equal to (SWIR – NIR) / (SWIR + NIR)

In the case of Landsat 5,7, NDBI is equal to float (Band 5 - Band 4)/float (Band 5 + Band 4)

In the case of Landsat 8, NDBI is equal to float (Band 6 - Band 5)/float (Band 6 + Band 5)

- NDVI is equal to (NIR – Red) / (NIR + Red)

In the case of Landsat 5,7, NDVI is equal to float (Band 4 - Band 3)/float (Band 4 + Band 3)

In the case of Landsat 8, NDVI is equal to float (Band 5 - Band 4)/float (Band 5 + Band 4)

- SAVI is equal to ((NIR - R) / (NIR + R + L)) * (1 + L)

In case of Landsat 5,7 SAVI is equal to float ((Band 4 – Band 3) / float (Band 4 + Band 3 + 0.5)) * (1.5).

In case of Landsat 8 SAVI is equal to float ((Band 5 – Band 4) / float (Band 5 + Band 4 + 0.5)) * (1.5).

The term "float" in the above formulas refers to floating-point, which is conceptually similar to scientific notation.

2.3.1 Steps involved in Retrieval of Urban Heat Island:

Step 1st: Convert the DN value to the at-sensor spectral radiance in the first step:

L is equal to $(L_{max} - L_{min}).Q_{cal} / (Q_{calmax} - Q_{calmin}) + L_{min} + O_i$

Where,

L_{max} is the maximum radiance in $Wm^{-2}sr^{-1}\mu m^{-1}$

L_{min} is the minimum radiance in $Wm^{-2}sr^{-1}\mu m^{-1}$

Q_{cal} is the pixel's DN value

Q_{calmax} is the highest pixel DN value.

Q_{calmin} is the minimum DN value of pixels

O_i is correction value of the thermal band

Step 2nd: $T = K_2/In\ (K_1/ L_\lambda+1) – 273.15$

Where,
T is At - Kelvin (K) values of the satellite for the brightness temperature.
L is spectral radiation at the TOA (watts/(m^2*ster*m)) at particular wavelength λ.
K_1 and K_2 are a constant for Band X, where X is the band number, and it stands for Band Specific Thermal Conversion from the Metadata.

Step 3rd: Calculation of Normalized Difference Vegetation Index (NDVI)
NDVI equals to (NIR – RED)/(NIR+RED)

Step 4th: Proportional vegetation (Pv) calculation:

P_V can be calculated as $((NDVI – NDVI_{min})/(NDVI_{max} – NDVI_{min}))^2$

Step 5th: Emissivity calculation:

$\varepsilon_\lambda = \varepsilon_{v\lambda} Pv + \varepsilon_{s\lambda} (1 - Pv)$

Where, P_V is the percentage of vegetation and ε_v and ε_s are the emissivities from the soil and vegetation respectively, at a given wavelength λ.

Step 6th: LST is equal to $BT/[1+\lambda*(BT/\rho)*In(\varepsilon)]$

Where, BT is brightness temperature, LST in degrees Celsius, ρ is (hc/σ) where σ being the Boltzmann constant (1.38×10^{-23} J/K), h being Plank's constant (6.626×10^{-34}), and c being the speed of light (3×10^8 m/s)

Step 7th: UHI is equal to (LST + δ)/2

Where, δ the land surface temperature's standard deviation.

After utilizing the above steps for generation of land cover indices and retrieval of urban heat island, 168 random points were generated in the region and due to rapid variations of land cover indices and heat intensity a logarithmic trend analysis were performed with the best fit curve R^2 and significance level *p*.

3. Result:

Section 3.1 The formulas provided in Section 2.3.1 have been used to derive indices, and the results are shown in the following figures with projection WGS_1984_UTM_Zone_44N as follows:

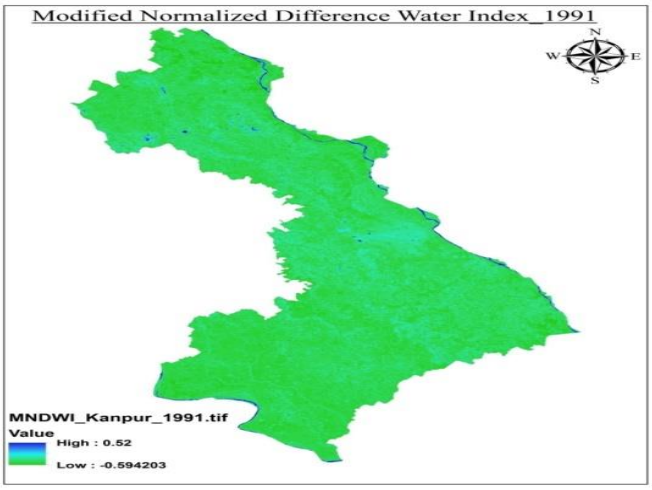

Figure 3.1.1(a)

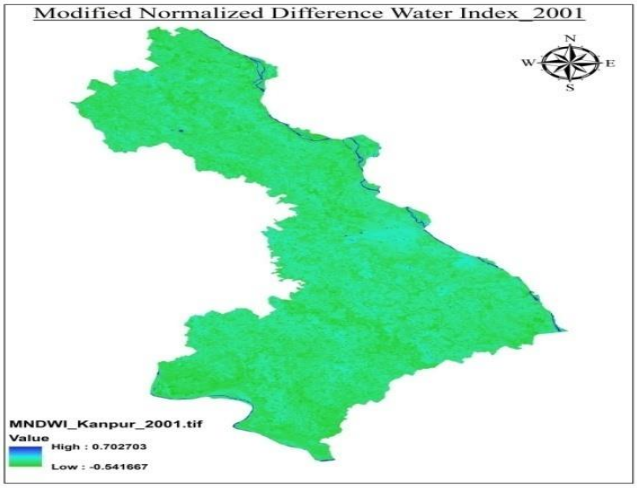

Figure 3.1.1(b)

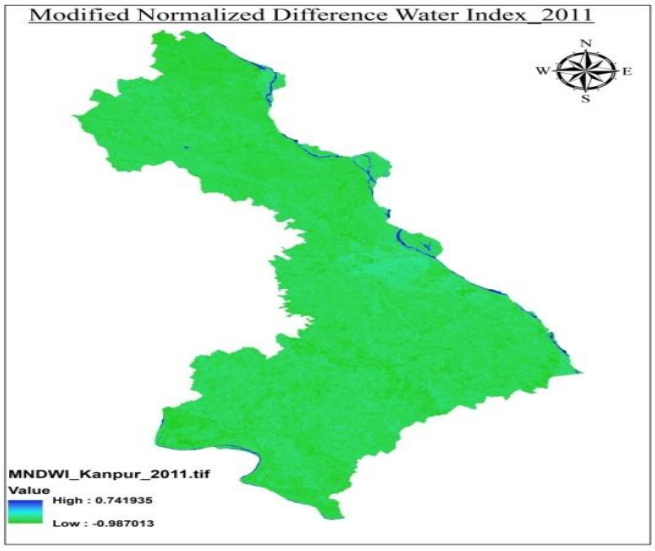

Figure 3.1.1(c)

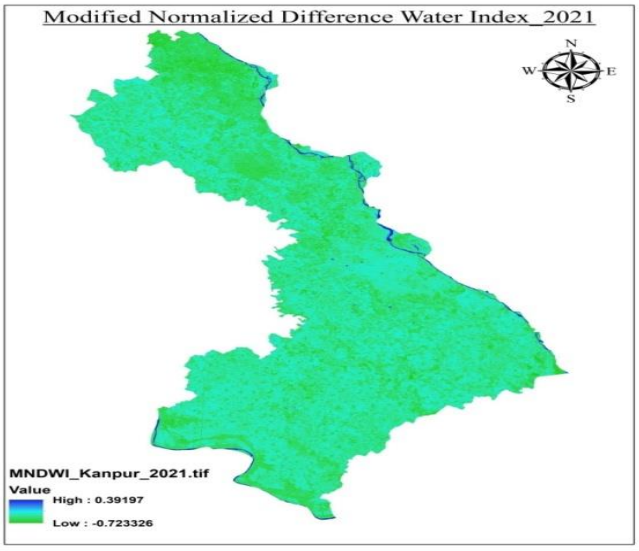

Figure 3.1.1(d)

The levels of water content in the study area for the years 1991, 2001, 2011 and 2021 are depicted in figures 3.1.1(a), 3.1.1(b), 3.1.1(c), and 3.1.1(d), respectively.

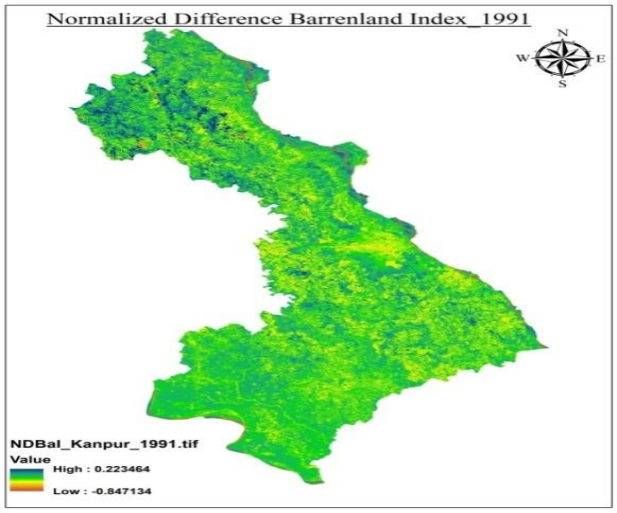

Figure 3.1.2(a)

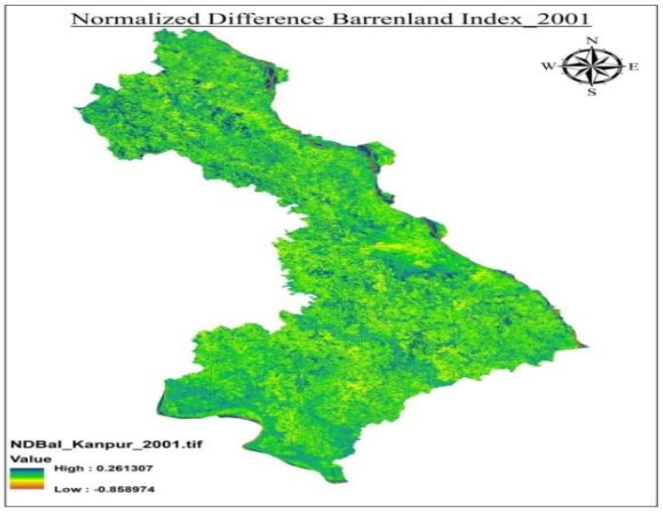

Figure 3.1.2(b)

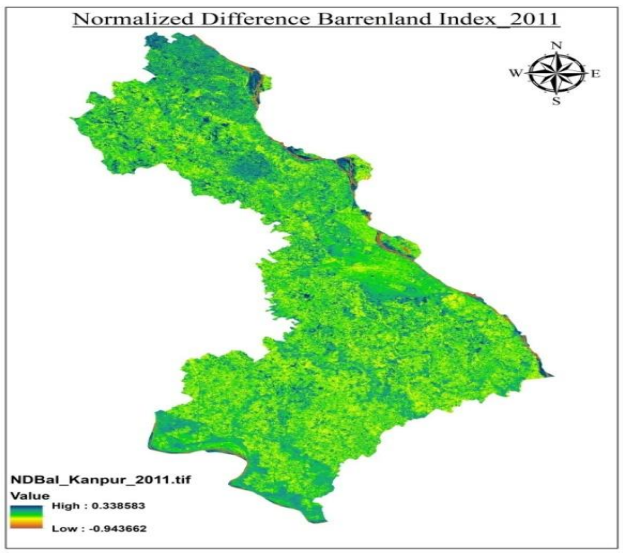

Figure 3.1.2(c)

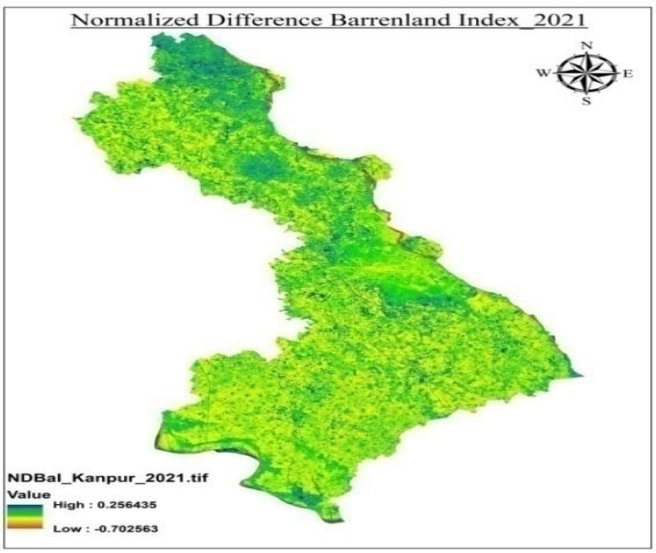

Figure 3.1.2(d)

Figures 3.1.2(a), 3.1.2(b), 3.1.2(c), and 3.1.2(d) depicts the intensities of barren land in the study area for the years 1991, 2001, 2011, and 2021 respectively.

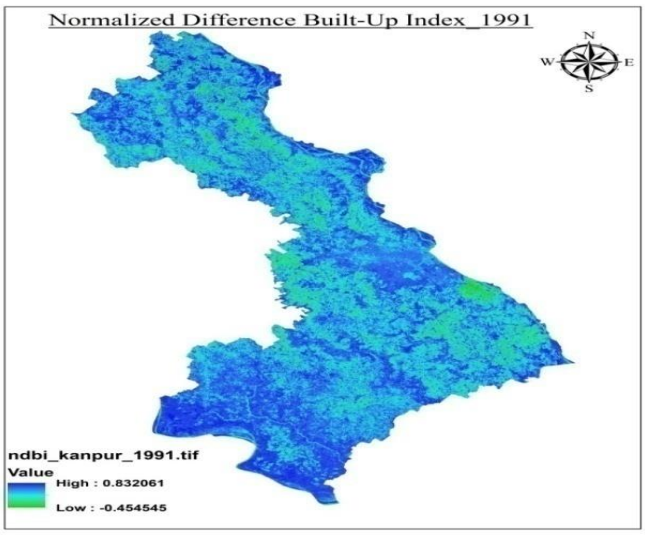

Figure 3.1.3(a)

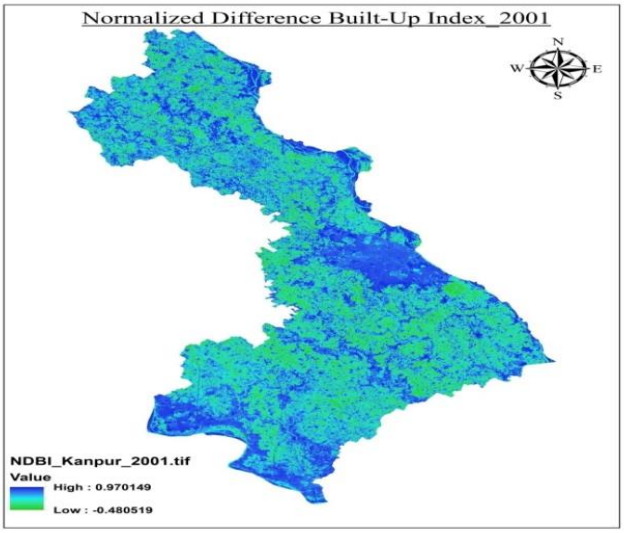

Figure 3.1.3(b)

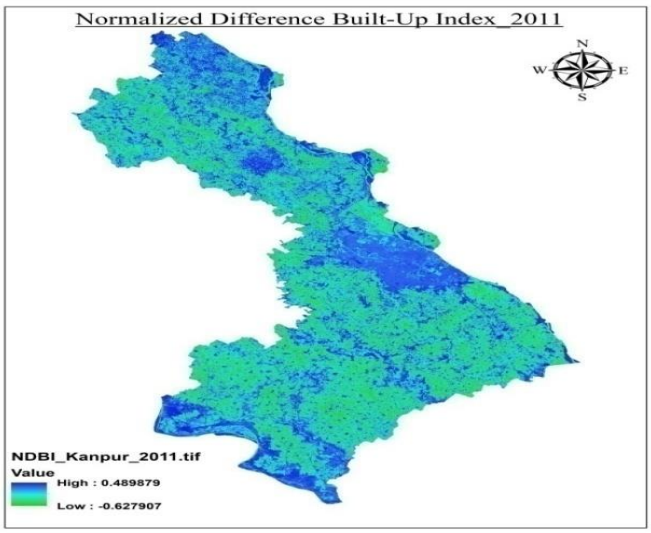

Figure 3.1.3(c)

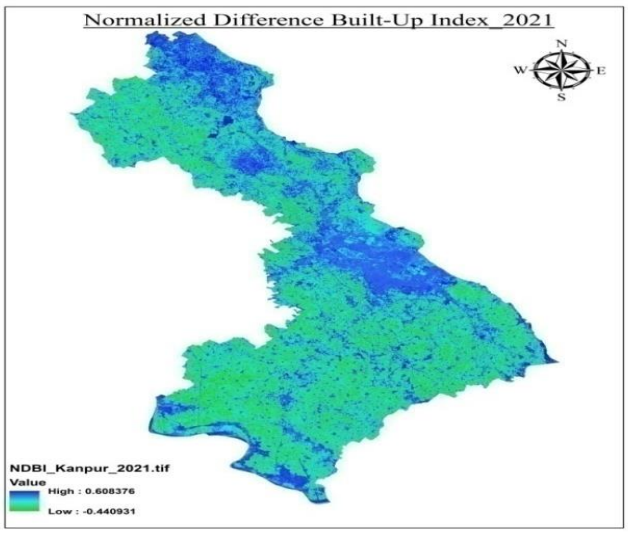

Figure 3.1.3(d)

The built-up intensities in the study area for the years 1991, 2001, 2011 and 2021 are depicted by figures 3.1.3(a), 3.1.3(b), 3.1.3(c), and 3.1.3(d), respectively.

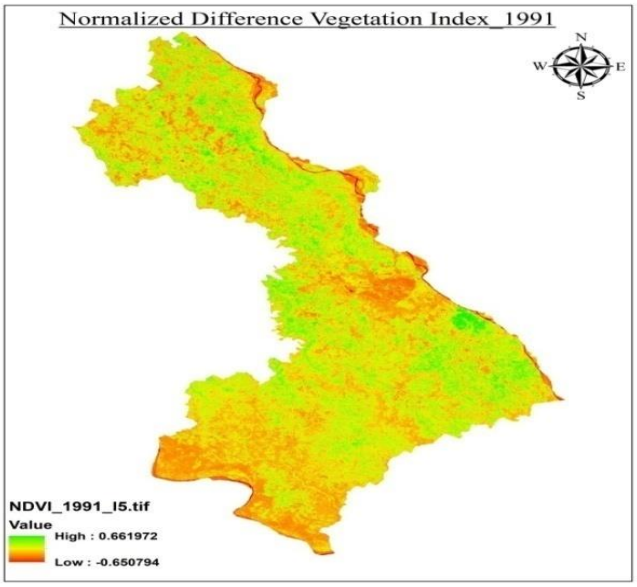

Figure 3.1.4(a)

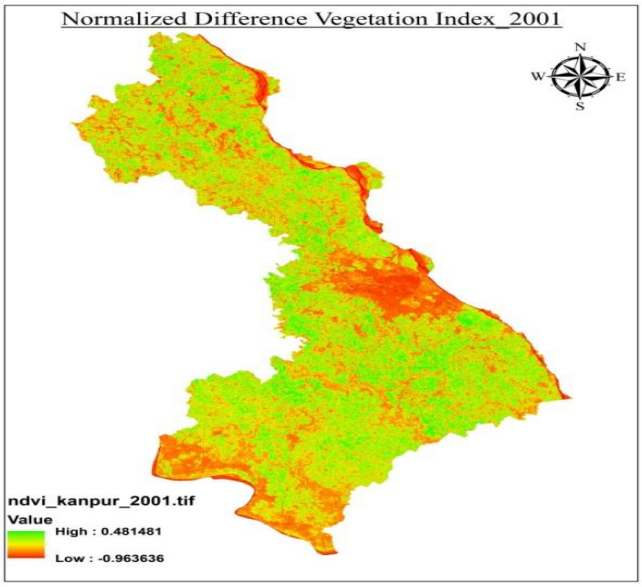

Figure 3.1.4(b)

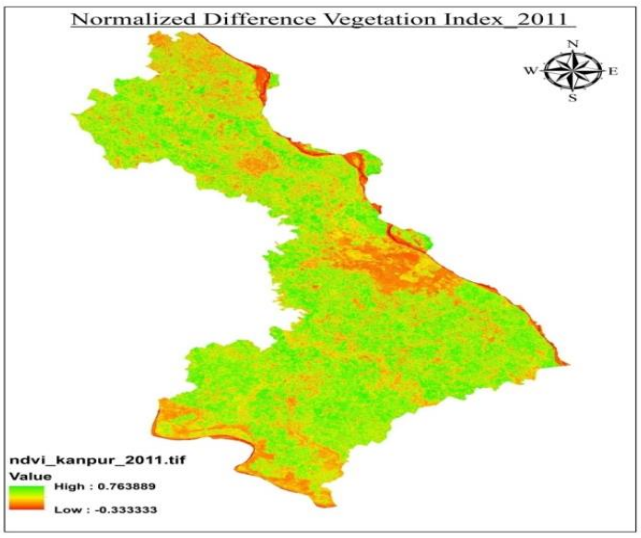

Figure 3.1.4(c)

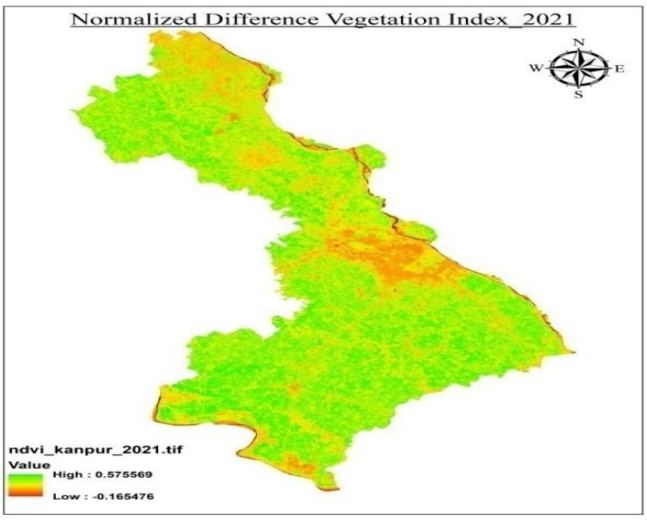

Figure 3.1.4(d)

The intensities of vegetation cover in the study area for the years 1991, 2001, 2011 and 2021 are depicted in figures 3.1.4(a), 3.1.4(b), 3.1.4(c), and 3.1.4(d), respectively.

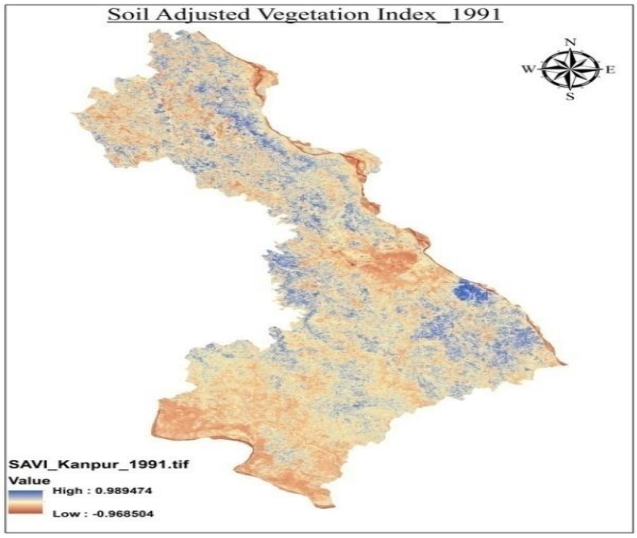

Figure 3.1.5(a)

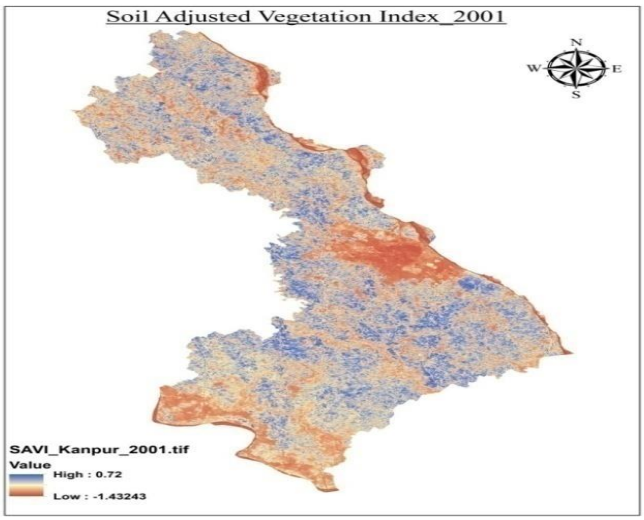

Figure 3.1.5(b)

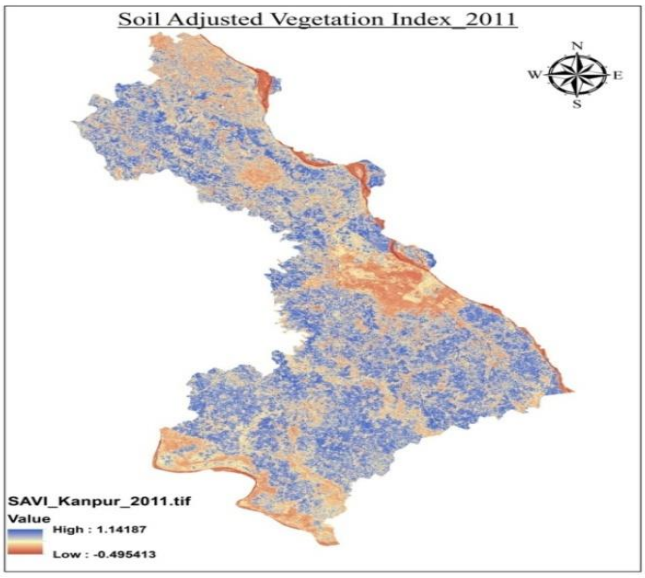

Figure 3.1.5(c)

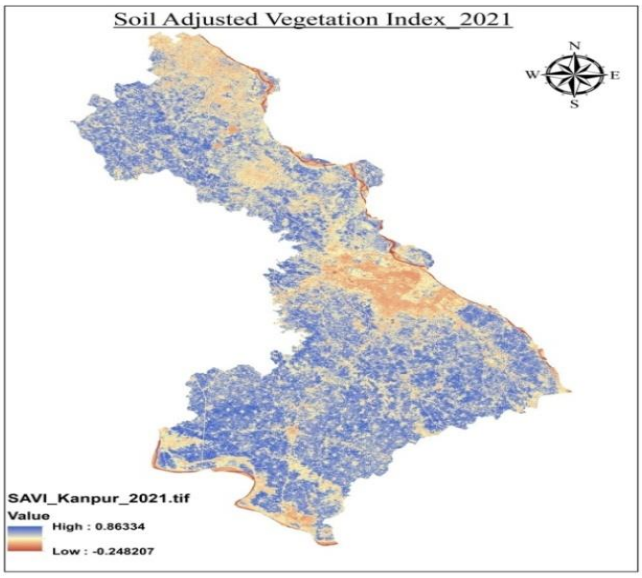

Figure 3.1.5(d)

The intensities of soil-adjusted vegetation in the study area for the years 1991, 2001, 2011 and 2021 are depicted in figures 3.1.5(a), 3.1.5(b), 3.1.5(c), and 3.1.5(d), respectively.

Section 3.2: The procedures and formulas described in Section 2.3.2 for Retrieving UHI Intensity have been used, and the following results for various years and bands have been discovered with the projection WGS_1984_UTM_Zone_44N.

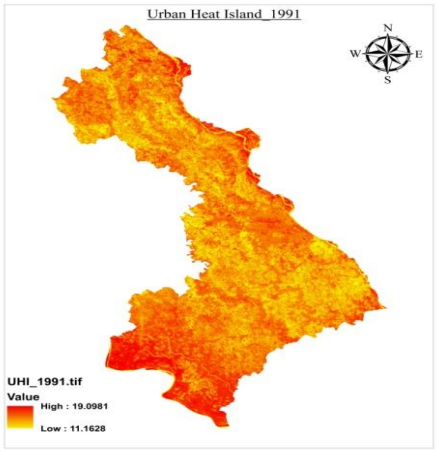

Figure 3.2(a)

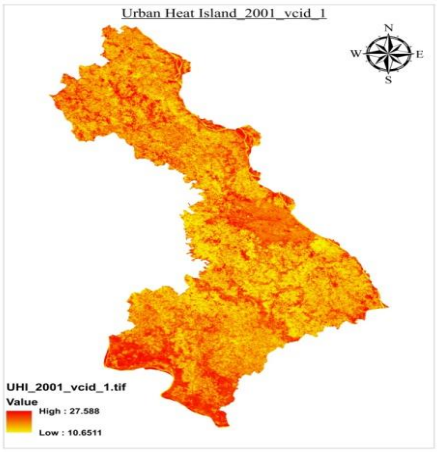

Figure 3.2(b)

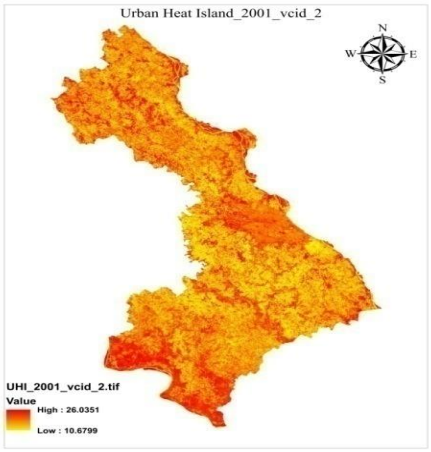

Figure 3.2(c)

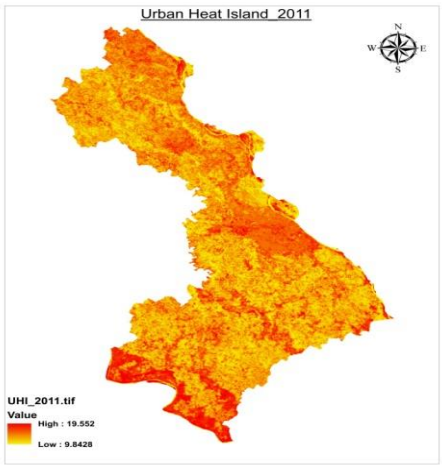

Figure 3.2(d)

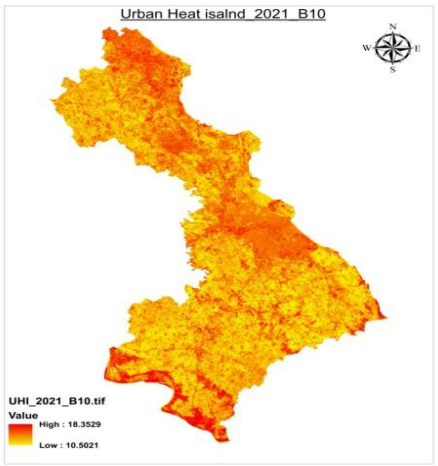

Figure 3.2(e)

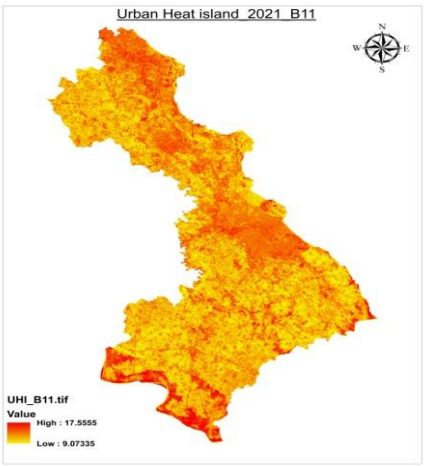

Figure 3.2(f)

The Surface Urban Heat Island Intensity (SUHII) for 1991 displays by Figure 3.2(a). Figures 3.2(b) and 3.2(c) display the SUHII for 2001, derived from vcid 1 and vcid 2 of the thermal band, respectively. Figure 3.2(d) displays the SUHII for 2011, while Figures 3.2(e) and 3.2(f) display the SUHII for 2021, derived from Band 10 and Band 11 respectively.

Section 3.3 The results are displayed in the graphs below, which show the relationship between various indices and Urban Heat Island Intensity at 168 randomly selected points from the study area.

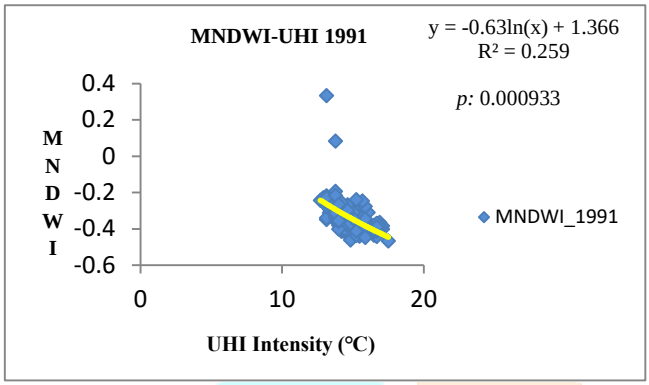

Graph 3.3.1(a)

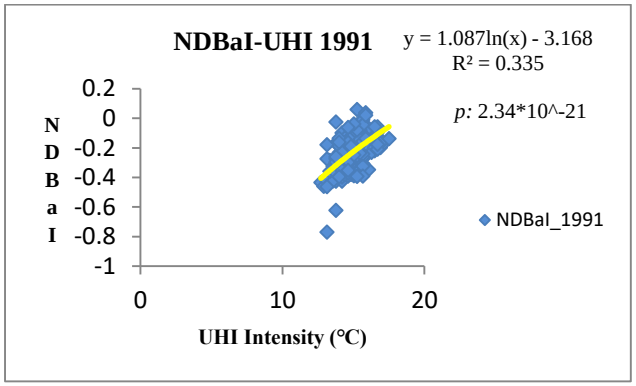

Graph 3.3.1(b)

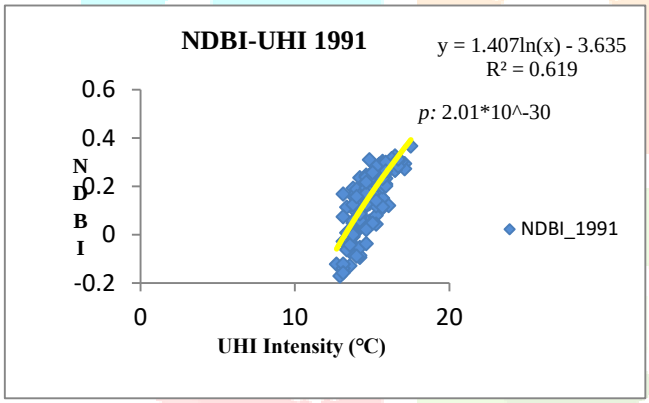

Graph 3.3.1(c)

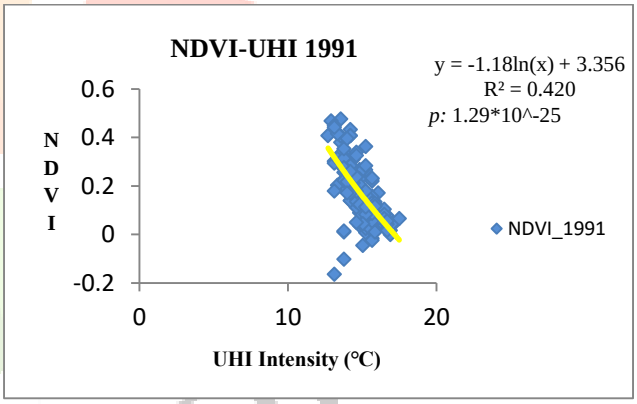

Graph 3.3.1(d)

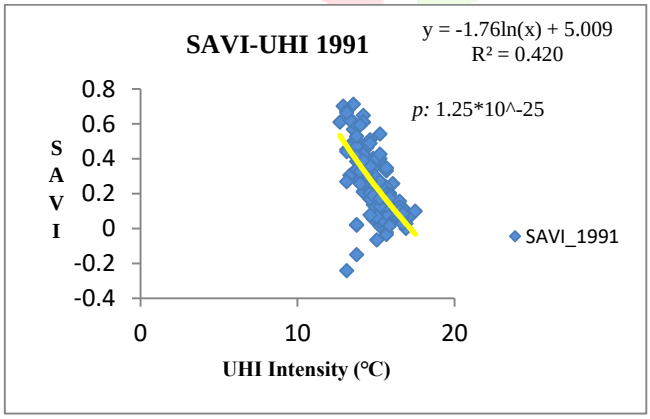

Graph 3.3.1(e)

In the graphs 3.3.1(a), 3.3.1(b), 3.3.1(c), 3.3.1(d), and 3.3.1(e), the relationship between MNDWI-UHI, NDBaI-UHI, NDBI-UHI, NDVI-UHI, and SAVI-UHI for the year 1991 is depicted. These graphs demonstrate that NDBI and UHI intensity have a high correlation that is positively skewed, whereas SAVI and UHI intensity have a high correlation that is negatively skewed, which suggests that the intensity of the urban heat island increases as built-up area increases while the intensity of the urban heat island decreases as shrub/grass area increases.

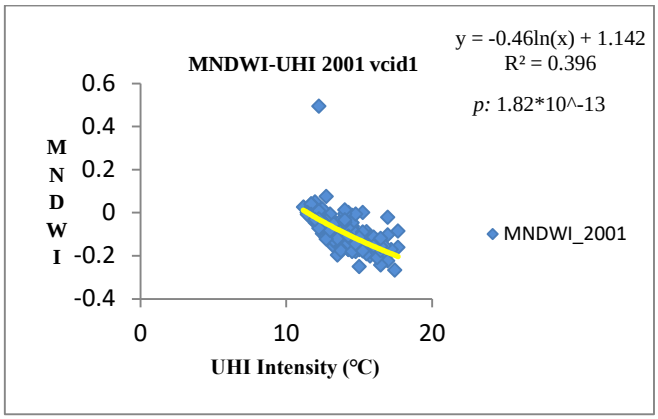

Graph 3.3.2(a)

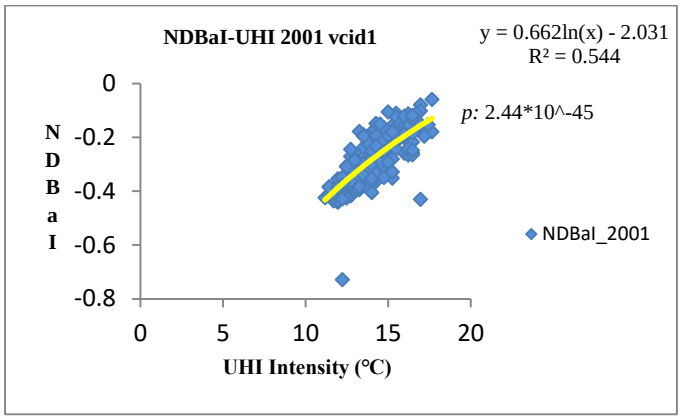

Graph 3.3.2(b)

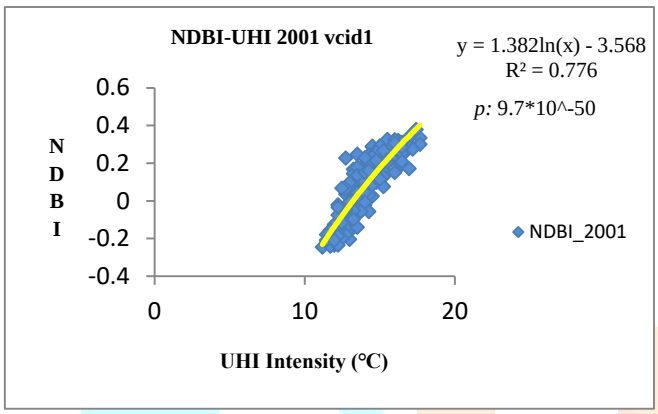

Graph 3.3.2(c)

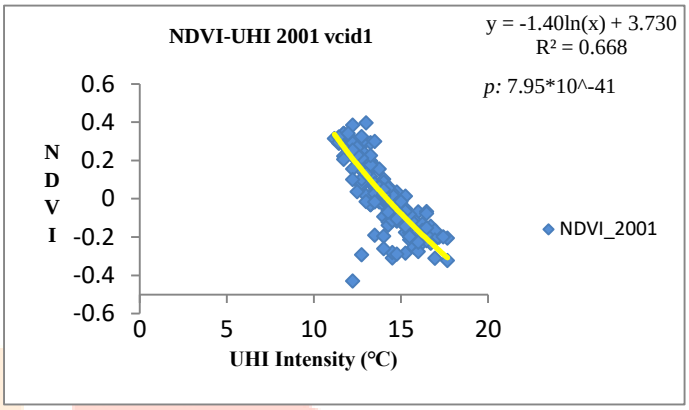

Graph 3.3.2(d)

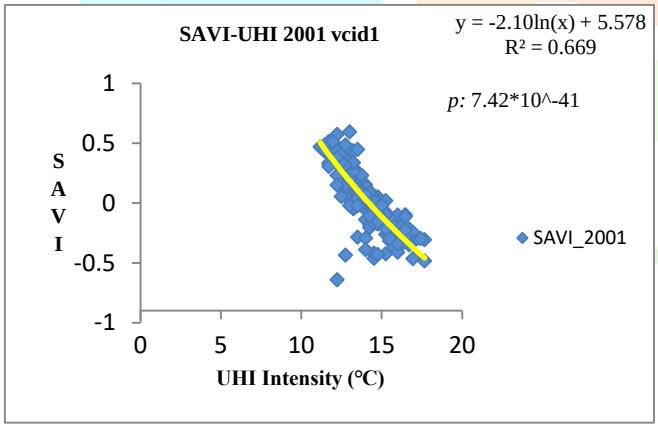

Graph 3.3.2(e)

The graphs 3.3.2(a), 3.3.2(b), 3.3.2(c), 3.3.2(d), and 3.3.2(e) show the relationship between MNDWI-UHI, NDBaI-UHI, NDBI-UHI, NDVI-UHI, and SAVI-UHI for the year 2001 (vcid 1 of thermal band), respectively. They demonstrate that NDBI and UHI intensity have a highly positive correlation, whereas SAVI and UHI intensity have a highly negative correlation which suggests that the intensity of the urban heat island increases as built-up area increases while the intensity of the urban heat island decreases as shrub/grass area increases.

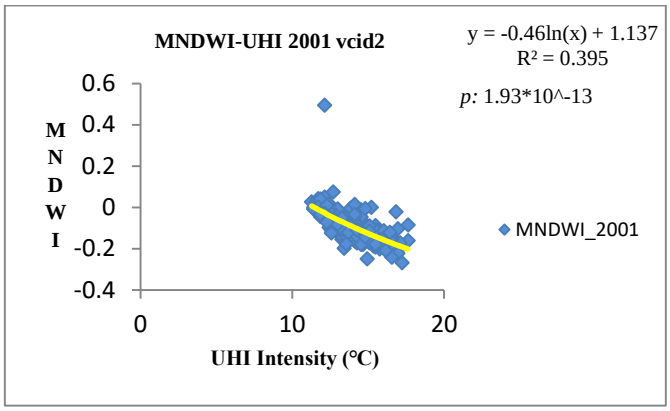

Graph 3.3.3(a)

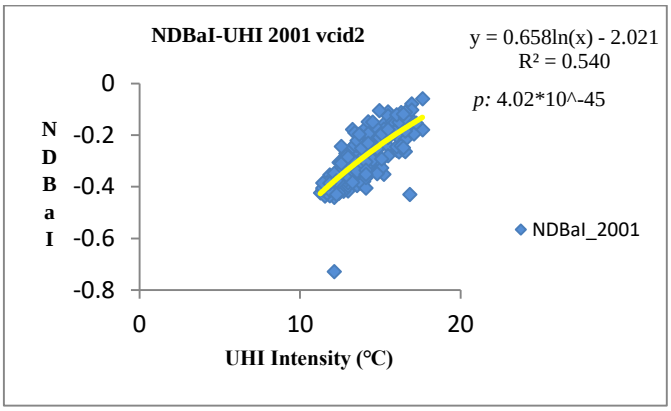

Graph 3.3.3(b)

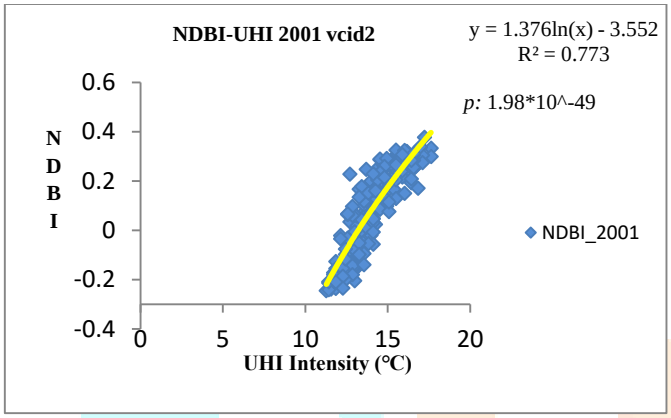

Graph 3.3.3(c)

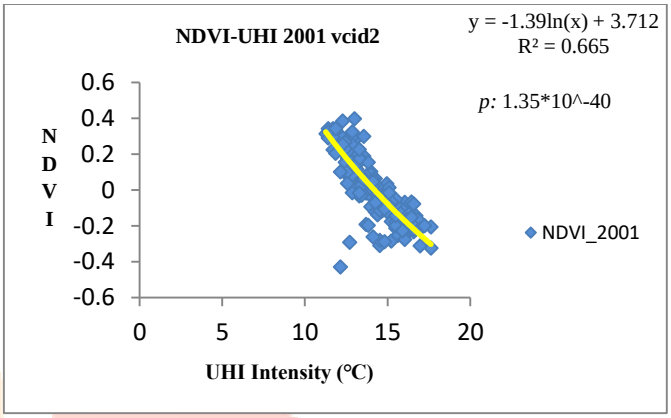

Graph 3.3.3(d)

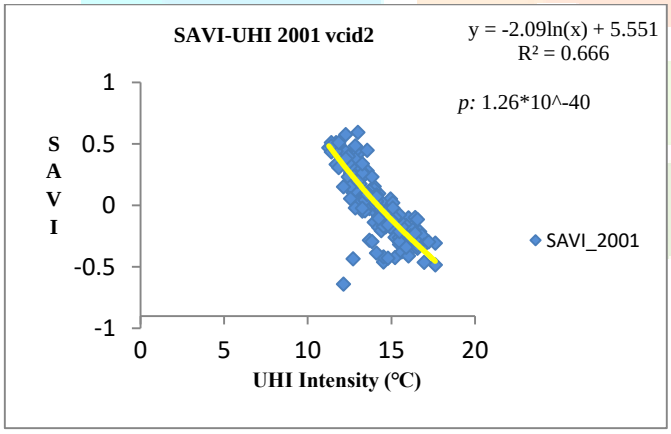

Graph 3.3.3(e)

The graphs in 3.3.3(a), 3.3.3(b), 3.3.3(c), 3.3.3(d), and 3.3.3(e) illustrate the relationship between MNDWI-UHI, NDBaI-UHI, NDBI-UHI, NDVI-UHI, and SAVI-UHI for the year 2001 (vcid 2 of thermal band), respectively. They demonstrate that NDBI and UHI intensity have a highly positive correlation, whereas SAVI and UHI intensity have a highly negative correlation which suggests that the intensity of the urban heat island increases as built-up area increases while the intensity of the urban heat island decreases as shrub/grass area increases.

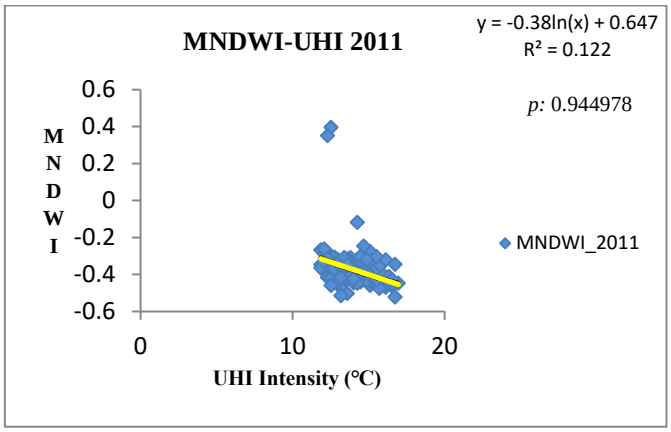

Graph 3.3.4(a)

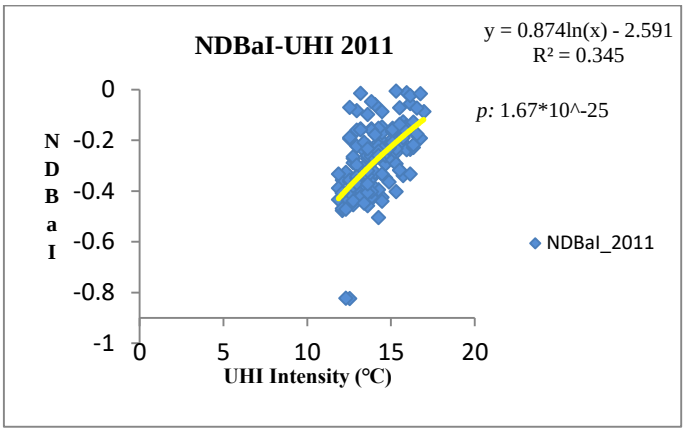

Graph 3.3.4(b)

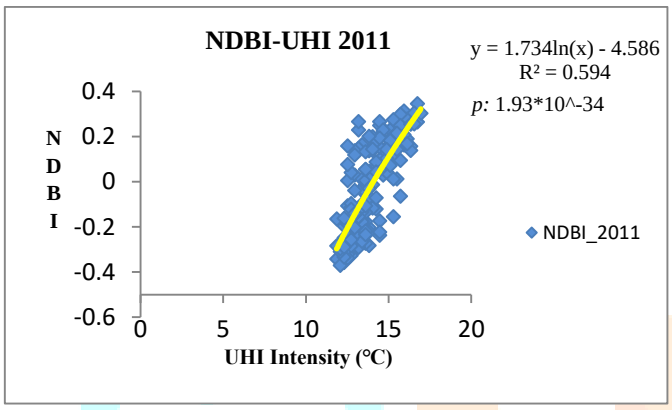

Graph 3.3.4(c)

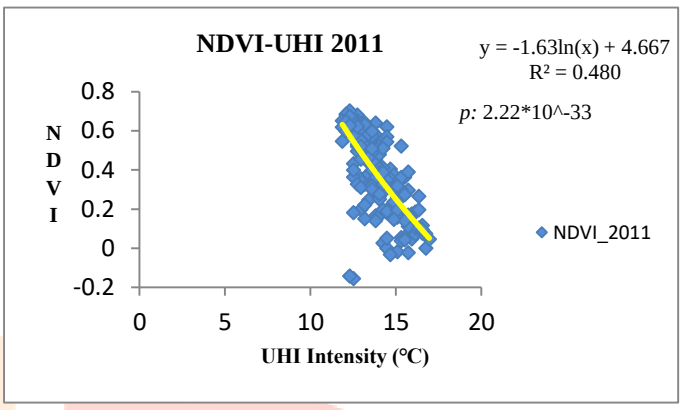

Graph 3.3.4(d)

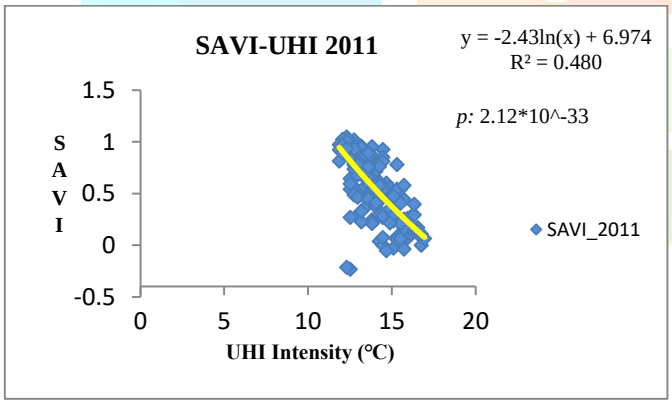

Graph 3.3.4(e)

The graphs 3.3.4(a), 3.3.4(b), 3.3.4(c), 3.3.4(d), and 3.3.4(e) show the relationship between MNDWI-UHI, NDBaI-UHI, NDBI-UHI, NDVI-UHI, and SAVI-UHI for the year 2011respectively. They demonstrate that NDBI and UHI intensity have a high correlation that is both positively and negatively skewed for SAVI and UHI intensity for the study area which suggests that the intensity of the urban heat island increases as built-up area increases while the intensity of the urban heat island decreases as shrub/grass area increases.

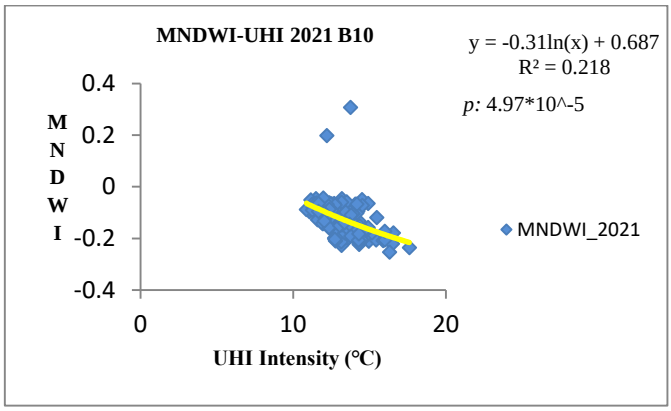

Graph 3.3.5(a)

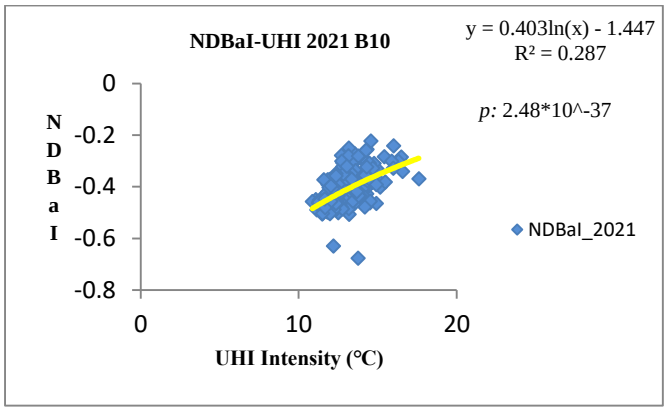

Graph 3.3.5(b)

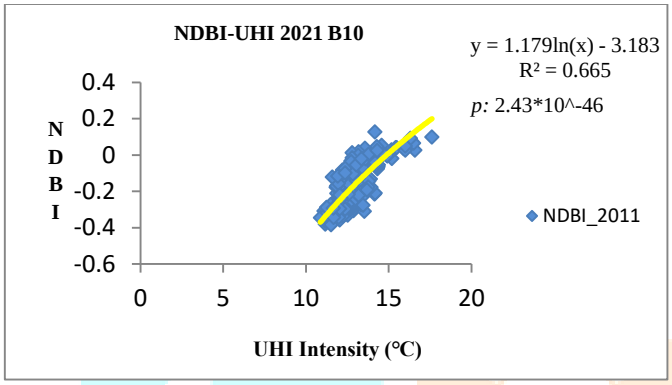

Graph 3.3.5(c)

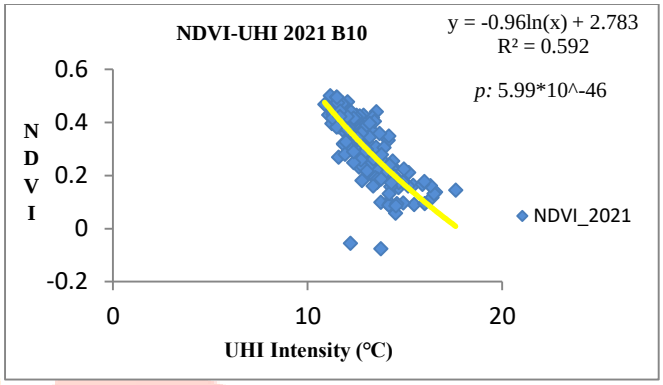

Graph 3.3.5(d)

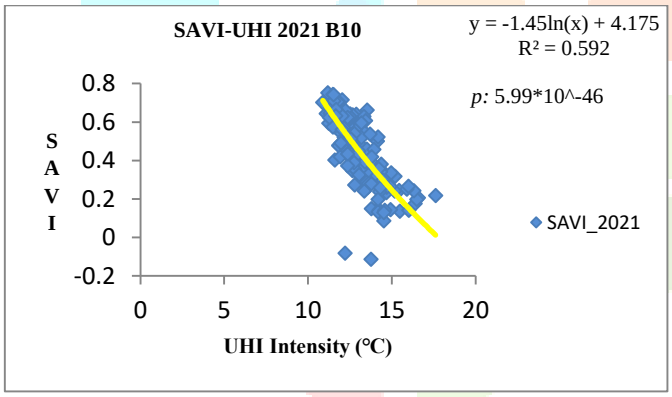

Graph 3.3.5(e)

For the year 2021 (for thermal band B10), the graphs in 3.3.5(a), 3.3.5(b), 3.3.5(c), 3.3.5(d), and 3.3.5(e) show the relationship between MNDWI-UHI, NDBaI-UHI, NDBI-UHI, NDVI-UHI, and SAVI-UHI, respectively. They demonstrate that there is a highly positive correlation between NDBI and UHI intensity while there is a highly negative correlation between SAVI and UHI intensity which suggests that the intensity of the urban heat island increases as built-up area increases while the intensity of the urban heat island decreases as shrub/grass area increases.

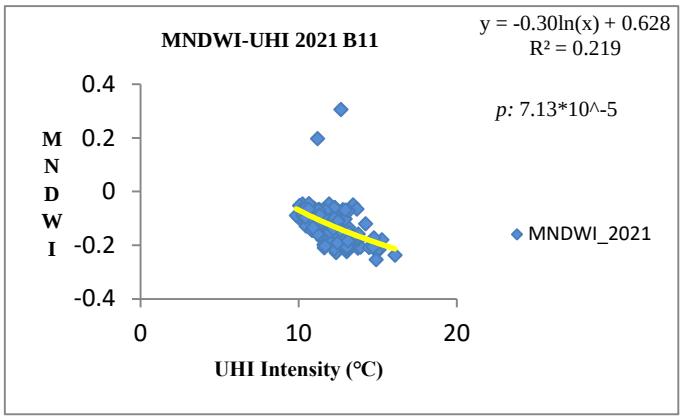

Graph 3.3.6(a)

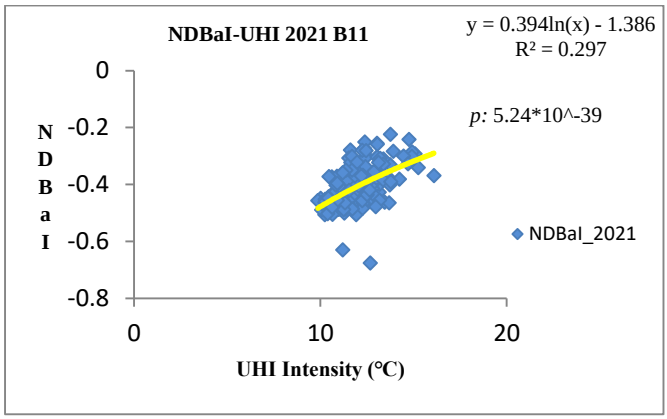

Graph 3.3.6(b)

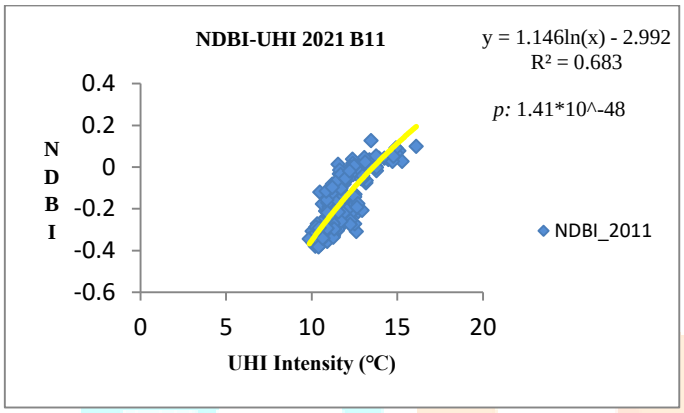

Graph 3.3.6(c)

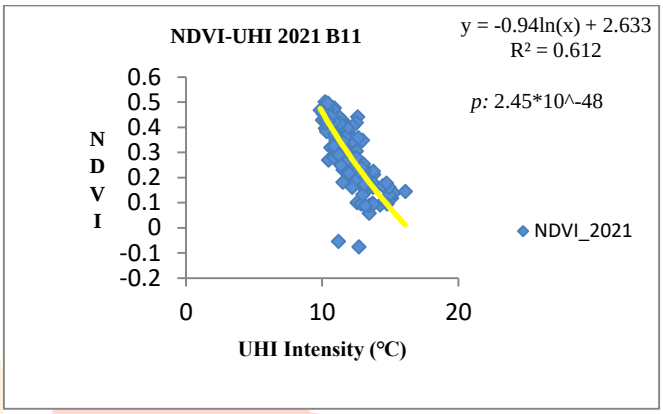

Graph 3.3.6(d)

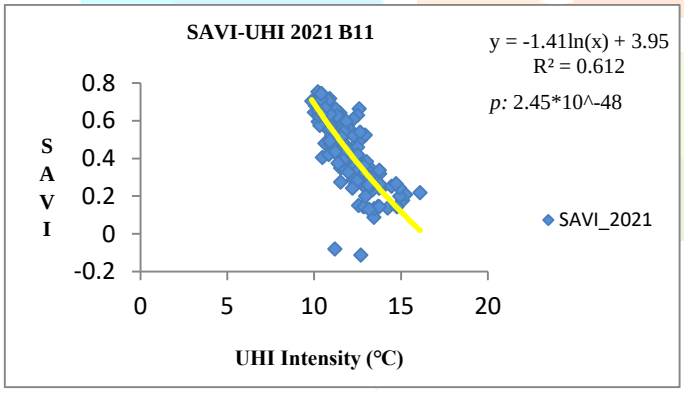

Graph 3.3.6(e)

In the graphs 3.3.6(a), 3.3.6(b), 3.3.6(c), 3.3.6(d), and 3.3.6(e), the relationship between MNDWI-UHI, NDBaI-UHI, NDBI-UHI, NDVI-UHI, and SAVI-UHI for the year 2021 (for thermal band B11) is depicted. These graphs demonstrate that NDBI and UHI intensity have a high correlation that is both positively and negatively skewed for SAVI and UHI intensity which suggests that the intensity of the urban heat island increases as built-up area increases while the intensity of the urban heat island decreases as shrub/grass area increases.

With very high significance level (i.e. *p*) ranging from $9.7*10^{-50}$ for 2001 vcid1 of band 6 to $2.01*10^{-30}$ for 1991, with gradient varying from 1.146 for 2021 Band 11 to 1.734 for 2011, data analysis has revealed that the Normalized Difference Built-up Index (NDBI) is highly positively correlated with Urban Heat Island (UHI) Intensity and Soil Adjusted Vegetation Index (SAVI) has a very strong negative correlation with Urban Heat Island (UHI) Intensity, with a very high significance level ranging from $2.45*10^{-48}$ for 2021 Band11 to $1.25*10^{-25}$ for 1991, and having gradient varies from 1.41 for 2021 Band11 to 2.43 for 2011.

Additionally, it is discovered that the Normalized Difference Barrenland Index (NDBaI) and Urban Heat Island (UHI) Intensity are positively correlated, with a high significance level ranging from $2.44*10^{-45}$ in 2001 to $2.34*10^{-21}$ in 1991, and a gradient varying from 1.087 in 1991 to 0.394 in 2021 Band 11 While the Modified Normalized Difference Water Index (MNDWI) is negatively correlated with Urban Heat Island (UHI) Intensity, the significance levels for the two variables range from $1.82*10^{-13}$ for 2001 vcid1 to 0.944978 for 2011, and the gradients between the two variables range from 0.30 for 2021 Band11 to 0.63 for 1991 With a significance level ranging from $2.45*10^{-48}$ for 2021 Band11 to $1.29*10^{-25}$ for 1991 and a gradient of 1.63 for 2011 to 0.94 for 2021 Band11, the Normalized Difference Vegetation Index (NDVI) is also negatively correlated with Urban Heat Island (UHI) Intensity.

R-squared value, which measures trendline reliability, is high for NDBI in the aforementioned graphs (ranging from 0.776 for 2001 vcid1 to 0.594 for 2011) and very low for MNDWI (ranging from 0.396 for 2001 vcid1 to 0.122 for 2011 This indicates that the MNDWI trendline fits UHI Intensity data the least, while the NDBI trendline fits UHI Intensity data better than other indices.

4.Discussion: In order to modify the area in accordance with these analyses, the decadal changes from 1991 to 2021 have been used to study the changes between these indices (MNDWI, NDBaI, NDBI, NDVI, SAVI) and urban heat island (UHI) Intensity The analysis also shows that the Shurb and Grass land region significantly reduces the Urban Heat Island (UHI) Intensity, which is good for the region's sustainable development. The Soil Adjusted has a very high negative impact on Urban Heat Island (UHI) Intensity, and it has a low to significant fit to the UHI data points. However, because the intensity of the Urban Heat Island (UHI) is greatly influenced by the Normalized Difference Built-up Index, which warms the area, it is possible to significantly reduce the intensity of the UHI by constructing green roofs and planting trees nearby (N.H. Wong et al., 2007; M. Fadhil et al., 2023). By increasing plantation/vegetation area and decreasing barren land area the Urban Heat Island (UHI) Intensity can also be decreased (Shweta Jain et al., 2020; M. Fadhil et al., 2023), which may also satisfy the Smart City concept for sustainable human development in this area and gives significantly advance further research projects based in India's Ganga-Yamuna Doab region as well as research processes nationwide.

5. Conclusion

Budgetary restrictions force the non-implementation of policies that result in improper urban planning and city development, which affects both city heat scenarios and land cover indices in developing countries like India. The relationship between various indices and urban heat intensity reveals a negative relationship between water bodies, vegetation, and shrub/grass land, while a positive relationship exists between bare land and built-up areas. Therefore, the development plans for Indian cities should take into account the relationships between various parameters and urban heat intensity. By properly implementing those plans, we can lessen the effects of urban heat in the cities, particularly in the Ganga-Yamuna Doab region of India.

Acknowledgement:

The authors are grateful to the University Grants Commission (UGC) and Principal of D.A.V. Degree College, Kanpur for providing the necessary facilities for the successful completion of this research. The first author wishes to acknowledge the support received from the Council of Scientific & Industrial Research (CSIR), New Delhi, India for providing grant under CSIR NET-JRF fellowship (Ref No.455/CSIR-UGC NET DEC. 2016).

Conflicts of Interest: There is no conflict of interest at all by all authors.

References:

1. Alademomi Alfred S. et al. (2020) Assessing the Relationship of LST, NDVI, EVI with Land Cover Changes in the Lagos Lagoon Environment. Quaestiones Geographicae 39(3) doi.org/10.2478/quageo-2020-0025
2. Almeida Catia Rodrigues de (2021) Study of Urban Heat Island (UHI) Using Remote Sensing Data/Techniques: A Systematic Review. Environments, 8(10) doi.org/10.3390/environments8100105
3. Aslan Nagihan et al. (2021) The Use of Land Cover Indices for Rapid Surface Urban Heat Island Detection from Multi-Temporal Landsat Imageries, 10(6), 416, doi.org/10.3390/ijgi10060416
4. Chakraborty T. et al. (2016) Understanding Diurnality and Inter-Seasonality of a sub-tropical Urban Heat Island. Boundary-Layer Meteorology, doi.org/10.1007/s10546-016-0223-0
5. Collins Jed et al. 2019 Urban Landscape Change Analysis Using Local Climate Zones and Object-Based Classification in the Salt Lake Metro Region, Utah, USA. Remote Sensing, 11(13) doi.org/10.3390/rs11131615
6. District Census Handbook, Kanpur Nagar 2011
7. Deng Chengbin and Changshan Wu (2012) BCI: A biophysical composition index for remote sensing of urban environments. Remote Sensing of Environment, 127,pp. 247-259
8. Duveiller, G., Hooker, J., & Cescatti, A. (2018). The mark of vegetation change on Earth's surface energy balance. Nature communications, 9(1), 679.
9. Fadhil M. et al. (2023) Mitigation urban heat island effects in the urban environments: strategies and tools. Earth and Environmental Sciences, 1129 (2023) 012025, doi.org/10.1088/1755-1315/1129/1/012025
10. Feng Dingrao et al. (2020) Do anthropogenic factors affect the improvement of vegetation cover in resource-based region?. Journal of Cleaner Production. 271, 122705. doi.org/10.1016/j.jclepro.2020.122705
11. Garcia David H. et al. (2023) Land Surface Temperature relationship with the Land Use/Land Cover Indices Leading to Thermal Field variation in the Turkish republic of Northern Cyprus.earth System and Environments, 7, pp. 561-580
12. Ghosh Subrata et al. (2018) Relation between urban biophysical composition and dynamics of land surface temperature in the Kolkata metropolitan area: a GIS and statistical based analysis for sustainable planning. Modeling Earth Systems and Environment, 5, 307-329
13. Grimmond C.S.B. and T.R. Oke (1998) Heat Storage in Urban Areas: Local Scale Observations and Evaluation of a Simple Model. Journal of Applied Metrology. Vol.38, pp. 922-940
14. Grover Aakriti and Ram Babu Singh (2015) Analysis of Urban Heat Island (UHI) in Relation to Normalized Difference Vegetation Index (NDVI): A Comparative Study of Delhi and Mumbai. Environments (2) 125-138, doi.org/10.3390/environments2020125
15. Hamoodi Mustafa et al (2017) Thermophysical behavior of LULC surfaces and their effect on the urban thermal environment. Spatial Sciences, 64(1), pp. 111-130, doi.org/10.1080/14498596.2017.1386598
16. Jain Shweta et al. (2020) Urban heat island intensity and its mitigation strategies in the fast-growing urban areas. Journal of Urban Management, 9(1), pp. 54-66 doi.org/10.1016/j.jum.2019.09.004
17. Joshi S. et al (2016) Developing Smart Cities: An Integrated Framework. Procedia Computer Science. 93, 902-909 doi.org/10.1016/j.procs.2016.07.258
18. Kumar Amit et al. 2021 Effect of Land Surface Temperature on Urban Heat Island in Varanasi city, India. Journal of Environmental Sciences, 4(3), pp. 420-429, doi.org/10.3390/j4030032
19. Kumar B.P. et al. 2023 Identification of climate change impact and thermal comfort zones in semi-arid regions of AP, India using LST and NDBI techniques. Journal of Cleaner Production, 407, pp.137-175 doi.org/10.1016/j.jclepro.2023.137175
20. Li Dan et al. (2020) Impact of land use land cover changes on regional climate in the Lhasa river basin, Tibetan Plateau. Science of the Total Environment 742(D12):140570 doi.org/10.1016/j.scitotenv.2020.140570

21. Li Hui et al. 2017 Mapping Typical Urban LULC from Landsat Imagery without Training Samples or Self-Defined Parameters. Remote Sensing 9, 700 doi.org/10.3390/rs9070700
22. Li Yunfei et al. (2020) On the influence of density and morphology on the Urban Heat Island Intensity. Nature Communications, 11(2647)
23. Masson, Valéry et al. (2020) Urban Climates and Climate Change Annual Review of Environment and Resources. 45 (1): pp.411–444, doi.org/10.1146/annurrev-environ-012320-083623
24. Rani Meenu et al. (2018) Multi-temporal NDVI and surface temperature analysis for Urban Heat Island inbuilt surrounding of sub-humid region: A case study of two geographical regions. Remote Sensing Applications: Society and Environment (10), pp.163-172, doi.org/ 10.1016/j.rsase.2018.03.007
25. Renard Florent et al. (2019) Evaluation of the Effect of Urban Redevelopment on Surface Urban Heat Islands. Remote Sensing, 11(3), 299 doi.org/10.3390/rs11030299
26. Singh Suraj Kumar (2016) Geospatial Technique for Land use/Land cover Mapping using Multi-Temporal Satellite Images: A case study of Samastipur District (India) Environ. We Int. J. Sci. Tech11 pp. 75-85
27. Sobrino José Antonio et al (2020) A Methodology for Comparing the Surface Urban Heat Island in Selected Urban Agglomerations Around the World from Sentinel-3 SLSTR Data. Remote Sensing 12 (2052) doi.org/10.3390/rs12122052
28. Serafin Stefano et al. (2018) Exchange processes in the Atmospheric boundary layer over Mountains Terrain. Atmosphere, 9(3), 102 doi.org/10.3390/atmos9030102
29. Stewart, Iain D. (2019). Why should urban heat island researchers study history?. Urban Climate. (30): 100484, doi.og/10.1016/j.unclim.2019, ISSN: 2212-0955
30. Ullah Waheed et al. (2023) Analysis of the relationship among land surface temperature (LST), land use land cover (LULC), and normalized difference vegetation index (NDVI) with topographic elements in the lower Himalayan region. Heliyon, 9(2), doi.org/10.1016/j.heliyon.2023.e13322
31. United Nations, Department of Economic and Social Affairs, Population Division (2019). World Urbanization Prospects: The 2018 Revision (ST/ESA/SER.A/420). New York: United Nations.
32. Wong N.H. et al. (2007) Environmental study of the impact of greenery in an institutional campus in the tropics. Building and Environment, 42(8), pp. 2249-2270
33. Yang Junyan et al. (2020) Impact of urban form on Thermal Environment near the surface region at pedestrian height: A case study based on High Density built-up areas of Nanjing city in China. Sustainability, 12(5) doi.org/10.3390/su12051737
34. Zhang Lei et al. (2022) Direct and indirect impacts of urbanization on vegetation growth across the worlds cities. Environmental Studies. 8(27), doi.org/10.1126/sciadv.abo0095
35. Zhang X.X. (2010) Relationship between vegetation greenness and urban heat island effect in Beijing City of China. Procedia Environmental Sciences, pp.1438-1450, doi.org/10.1016/j.proenv.2010.10.157
36. Zhao Q, Wen Z, Chen S, Ding S, Zhang M. (2019) Quantifying Land Use/Land Cover and Landscape Pattern Changes and Impacts on Ecosystem Services. Int J Environ Res Public Health. 17(1):126, doi.org/ 10.3390/ijerph17010126. PMID: 31878063; PMCID: PMC6981947.